A01-25033

42nd AIAA/ASME/ASCE/AHS/ASC Structures, Structural Dynamics, and Materials Conference and Exhibit
Seattle, WA 16-19 April 2001

AIAA-2001-1219

Facesheet Push-off Tests to Determine Composite Sandwich Toughness at Cryogenic Temperatures [1]

Thomas S. Gates* and Helen M. Herring+
NASA Langley Research Center, Hampton VA 23681

Abstract

A new novel test method, associated analysis, and experimental procedures are developed to investigate the toughness of the facesheet-to-core interface of a sandwich material at cryogenic temperatures. The test method is designed to simulate the failure mode associated with facesheet debonding from high levels of gas pressure in the sandwich core. The effects of specimen orientation are considered, and the results of toughness measurements are presented. Comparisons are made between room and liquid nitrogen (-196°C) test temperatures. It was determined that the test method is insensitive to specimen facesheet orientation and strain energy release rate increases with a decrease in the test temperature.

Introduction

Future space transportation vehicles will require lighter weight structures to meet the increased demands on performance. One area identified as a potential source for significant weight reduction is the replacement of metallic cryogenic fuel tanks with polymeric matrix composite (PMC) tanks. A promising structural concept based on PMC materials is to use a sandwich construction with the PMC as the facesheet material and lightweight polymeric materials as the core. As outlined extensively by [1], the sandwich construction technique has many advantages over typical stiffened skin concepts, not the least of which is reduced weight. However, sandwich construction has a number of potential problems because the presence of multiple interfaces serves as a source for failure initiation and growth.

The interest in design of polymeric composite cryogenic-fuel tanks for spacecraft goes back several years to the research associated with the National Aerospace Plane (NASP) and the single-stage-to-orbit (SSTO) vehicles [2]. These studies addressed weight and cost benefits as well as the complex technical issues such as fatigue crack resistance and oxidation-corrosion resistance. It was recognized that permeation resistance of the tanks could be the overriding design criteria. Concepts were proposed for both the liquid-oxygen tanks and the liquid-hydrogen tanks.

In 1996, the DC-XA suborbital demonstration vehicle was built with an all-composite liquid-hydrogen fuel tank [3]. That tank was designed as an unlined, unstiffened cylinder measuring approximately 2.4m in diameter. The tank performed as expected in both ground and flight tests.

For integrated cryogenic tank, the tank wall materials must carry structural and pressure loads while operating over an extremely wide temperature range. One possible failure mechanism, associated with the use of sandwich materials in such a demanding environment, is cryopumping that occurs during repeated cryogenic fluid fill and drain cycles. Cryopumping is the influx of gas into an unclosed volume resulting from the vacuum generated when cryogenic temperatures liquefy and condense the gas on the boundaries of that volume. This cryopumping will occur when the tank wall facesheet(s) develop leaks and allow the cryogen to permeate into the core. Subsequent warming of the cryogen causes a transition from a liquid to a gas phase and results in a substantial increase in core pressure. Without proper venting of this pressure, the core, facesheet, and bondline must sustain the resultant pressure loads without failure. The most likely

---

* Senior Materials Research Engineer, Mechanics and Durability Branch, Associate Fellow, AIAA.
+ Research Scientist, Analytical Services and Materials

initial failure mode due to cryopumping is facesheet-to-core debonding that can lead to crack growth and a total separation of the facesheet.

This failure mode occurred recently in the NASA X-33 reusable flight demonstration vehicle. The X-33 was designed with a large, (8.7 x 6.1 x 4.3 meter) conformal tank made from a sandwich construction of polymeric composite skins and phenolic core. After successful completion of the first protoflight pressure and loads test, the tank was drained of its liquid hydrogen fuel, and a purge of the tank began. Approximately 15 minutes after the tank was drained, the outer facesheet and core separated from the inner facesheet along part of the tank wall [4]. It was subsequently determined that many factors contributed to the tank failure. Considering the mechanics of the failure, it was found that the inner tank wall allowed permeation by way of microcracks in the facesheet. As pressure and strain decreased below that required to sustain the microcrack paths, the leak paths closed. As the tank warmed, the remaining trapped cryogens proceeded to vaporize, creating high pressure (cryopumping). This pressure, coupled with bondline defects, likely caused the failure. Failure or debonding occurred almost exclusively at the core-to-adhesive surface on the inner facesheet side.

The new, novel test method was designed to simulate the failure mode associated with facesheet debonding in the presence of pressure in the sandwich core. The present paper provides details on the material, test fixtures, and test specimen design. Fracture analysis based on the compliance calibration method is outlined and the process for conversion of test data to strain energy release rate is provided. The effects of test temperature and test specimen orientation are discussed.

Material and Test Specimens

The test specimen was a typical sandwich construction made from a complex arrangement of composite facesheets, adhesive, and honeycomb core materials. The test method was based on a three-point bend approach relying on the sandwich beam to react the bending load.

Materials

The test material for this study was taken from a section of an X-33 liquid-hydrogen fuel tank. These tank walls were made into large, curved panels joined to form the complete tank structure. The material was a sandwich construction with an aramid-phenolic based core and graphite-fiber, polymeric composite facesheets.

The facesheet material was IM7/977-2, and as shown in Fig. 1, the two facesheets had distinct layups. In order to explore the effect of facesheet orientation on the facesheet debonding, small test specimens were cut in two directions from larger panels. For reference purposes, the *longitudinal* direction was defined as the direction parallel to the 0^0 plies and the *transverse* direction was defined as the direction parallel to the 90^0 plies. The *inner* facesheet was defined as the laminate on the inside of the tank wall (closest to the cryogen) and the *outer* facesheet was defined as the laminate on the outer-wall surface.

The inner facesheet was 13 plies thick and was pre-cured prior to the build-up of the sandwich. The facesheet tension modulus and coefficient of thermal expansion (CTE) are given in Table 1.

Both the inner and outer facesheet were bond cured to the core using AF-191 film adhesive. The outer facesheet was 7 plies and co-cured on the inner facesheet/core assembly. The modulus and CTE for this facesheet are also given in table 1.

The core material was unvented Korex and was manufactured in a regular hexagonal pattern. Fig. 2 shows the relevant dimensions of the core. The average area of the core hexagon was estimated to be 23.2 mm^2. The core "ribbon" direction is shown in Fig. 2 and corresponds to the facesheet longitudinal direction.

Using the definitions provided by [1], the relative density of the core is calculated from

$$\rho^*/\rho_s = \frac{(t/l)\left(h/l + 2\right)}{2\cos\theta\left(h/l + \sin\theta\right)} \qquad (1)$$

where ρ^* and ρ_s are the honeycomb-core density and density of core base material, respectively. As shown in Fig. 2, for the following dimensions,

$$\theta = 30^0,\ h = l = 3.24mm,\ t = 0.15mm$$

give a relative core density of 0.053. Defining the coordinates directions for the core to be (1,2,3) where (1,2) are in the plane of the hexagon (Fig. 2) and (3) is out of the plane, and using the superscript * and the subscript s to define the honeycomb and base material, respectively, expressions for directional modulus (E) are found from [1].

$$\frac{E_1^*}{E_s} = \frac{E_2^*}{E_s} = 2.3\left(t/l\right)^3 \ll 0 \qquad (2)$$

Equation 2 implies a very low relative stiffness of the core for in-plane loading. For out-of-plane loading, [1]

provides the formula to estimate the relative, out-of-plane stiffness, that is,

$$\frac{E_3^*}{E_s} = \frac{\rho^*}{\rho_s} = .053 \qquad (3)$$

	Modulus (tension) (Gpa)		CTE * ($x10^{-6}$ mm/mm/^{0}C)	
	Long.	Trans.	Long.	Trans.
Inner, RT	49.6	80.5	3.6	2.3
Outer, RT	58.3	86.9	2.9	1.1
Inner, -253^{0}C	53.4	86.3		
Outer, -253^{0}C	62.5	93.2		

* Coefficient of thermal expansion measured between -100^{0}C and +160^{0}C

Table 1. Measured material properties of inner and outer facesheets.

Fracture Test Specimens

Fracture tests were conducted on rectangular specimens of the sandwich material. As shown in Fig. 3, the tests specimens were cut into a beam shape with the overall dimensions of 152 x 25.4 x 31.2 mm. The intent of the fracture tests was to debond the inner facesheet by growing a crack along the core/adhesive/facesheet interface region. Figures 3 and 4 illustrate the position of the specimen relative to the test fixture. To provide space for the center load bar, each test specimen had a 25.4 mm diameter through-hole cut in the specimen adjacent to the inner facesheet at the midpoint of the length. To facilitate the growth of the crack, a starter crack was cut across the width on each side of the hole with a thin saw blade to approximately one cell depth along the facesheet-to-core interface.

Push-Off Test Fixture

As illustrated in Fig. 3 and the photograph of Fig. 4, a unique test fixture was developed to perform the facesheet push-off fracture tests. The basic concept is to use a three-point bend apparatus that loads the facesheet from inside the sandwich beam and grows a crack along the interface region of the core, adhesive, and facesheet. The applied load is reacted at the ends of the beam by circular rods acting as simple supports. A stiff base plate then supports the whole apparatus.

Fracture Analysis

The influence of temperature on the strain-energy release rate for laminated composite materials has been examined in a couple of recent studies. In one study [5], the tests were performed on an epoxy based composite material using the double cantilever beam (DCB) specimen. It was found that the value of strain-energy release rate (G), (Mode I) increased approximately two-fold when the test temperature was lowered from room temperature to -196^{0}C. In a similar study, [6] found the value of G (Mode I, DCB specimen) for the material IM7/977-3 decreased when the temperature was lowered from room temperature to -196^{0}C by a factor of approximately 1.5. These somewhat conflicting studies indicate that additional work may be required to standardize toughness tests at cryogenic temperatures for laminated materials.

During repeated flights, the cryogenic-fuel tanks are expected to survive extended use. During these flights, it is also expected that some leakage or permeation of cryogen through the tank walls will occur. The extent and severity of this leakage will be a function of many factors including material type, construction techniques, thermal and mechanical loads, and damage initiation and growth.

One failure scenario assumes that the inner facesheet of the sandwich sustains enough damage to allow measurable cryogen leakage into the core that subsequently leads to a build-up of high-pressure inside the sandwich during warming of the tank. One critical and potentially catastrophic failure mode associated with the build-up of internal pressure in the core material is fracture along the facesheet-to-core interface, and the subsequent push-off of one or both of the facesheets.

The intent of the push-off test method is to simulate this failure mode by growing a crack in the interface region. Measuring the associated applied load and calculating the critical strain-energy release rate, or fracture energy as a function of crack length, allowed for the calculation of the fracture energy associated with the crack growth. It was assumed that the fracture mode was predominately Mode I for this test.

The analysis method, outlined here, is based on the compliance calibration method, or Berry's method as given by [7] and [8]. Additional information on this method and other types of Mode I fracture tests can be found in [9].

Compliance

The calculated compliance of the test specimen is based on the load and displacement measurements during test. The compliance is given by,

$$C = \frac{P}{\delta} \qquad (4)$$

where C is compliance, P is load and δ is the transverse displacement at the point of load application. Specimen compliance is then related to crack length through an empirical relationship,

$$C = ba^m \tag{5}$$

where a is the crack length and b, m are empirical constants determined through a linear fit to a double logarithmic plot of C versus a.

Strain-Energy Release Rate

In general, the critical strain-energy release rate is a function of the strain energy and crack length

$$G_c = \frac{dU}{da} \tag{6}$$

where G_c is the strain-energy release rate and U is the strain energy. For a specimen of width w, Eq. (6) gives

$$G_c = \frac{P\delta}{2wC}\frac{dC}{da} \tag{7}$$

and then using Eq.s (4) and (5) the critical strain-energy release rate becomes

$$G_c = \frac{P^2}{2w}\left(mba^{(m-1)}\right) \tag{8}$$

From this last equation, the critical strain-energy release rate is calculated by using the four experimentally determined parameters: m, b, a, and P.

Test Plan

The test plan was constructed to investigate the fracture toughness as a function of two variables; that is, temperature and specimen orientation. The two test temperatures investigated were; room temperature (23^0C) and cryogenic temperature (-196^0C) (LN_2). The two specimen orientations investigated were longitudinal and transverse, where the orientations were defined previously. At least 3 replicates for each test condition were used to develop the final data.

Experimental Methods and Procedures

The use of the novel test presented herein required development of new experimental methods and data-reduction procedures. The test methods fall into one of two broad categories; facesheet push-off and debond crack measurement.

Push-Off Test

The push-off test was run in a servo-hydraulic test machine using displacement control at a rate of 0.0254mm per second. Load, as measured by the test machine load cell, and displacement, as measured by the test machine transducer, were monitored and recorded as a function of test time at a sampling frequency of 0.25 Hz.

By adjusting the starting position of the actuator, the initial applied load for each test was kept at zero. A typical test run had several distinct sections or events that are illustrated in the typical load-versus-displacement data of Fig. 5. During the loading phase of a test, the load-versus-displacement curve was approximately linear until the crack started to grow.

Due to the nature of the crack growth in the honeycomb/facesheet interface, the major portion of crack growth would occur suddenly accompanied by a significant and fast reduction in load. At this point in the test, the test operator would initiate a controlled reversal in displacement that would result in unloading of the test specimen.

The unloading phase had two distinct portions that were distinguished by an abrupt change in the slope of the load-versus-displacement curve. This abrupt change is also illustrated in Fig. 5. The compliance, as given by Eq. (4), was determined from this final unloading portion of the curve. The effective crack length, calculated using the procedures described below, was then plotted as a function of compliance on a double logarithmic scale and fit with Eq. (5) as illustrated by the example data presented in Fig. 6.

In general, the crack growth associated with such a test run would be small but measurable and would represent some fraction of the total bonded area. In order to quantify the crack length as a function of load and displacement, this typical test run would then be repeated 3 to 5 times or until the crack approached to within approximately 25mm of the reaction rollers. Load versus displacement data for a typical series of test runs is given in Fig. 7.

For the room temperature tests, the push-off apparatus was used as depicted in Fig. 4. For the cryogenic tests, the apparatus was placed in an aluminum vessel that was filled with liquid nitrogen prior to the start of the test run. As shown in the schematic of Fig. 3, the apparatus and test specimen remained submerged in the liquid nitrogen (-196^0C) during the course of the test run. The tests that were submerged in liquid nitrogen offered no opportunity to view a debond or crack during the test run and hence the only real-time data on crack growth was obtained by observance of a significant load reduction event.

Crack Measurement via X-ray Inspection

The crack, which developed during the course of loading, was quantified by calculating an effective crack length based on the number of debonded cells. To quantify this debond, the specimen was removed from the test fixture after each run and examined by an x-ray radiography method. Briefly, this method consisted of injecting a small amount of dye penetrate into the crack on both sides of the center hole and then subjecting the

specimen to a focused x-ray in the through-the-thickness direction. As shown by the typical x-ray images in Fig. 8, the debonded cells appeared as dark regions on the image and were easily distinguishable. As illustrated in Fig. 8, the center section of each specimen was where the cut-out was made to accommodate the load bar.

With an accurate count of debonded cells established, an effective crack length was then calculated using

$$\bar{a} = \frac{A_c n_{DB}}{w} \tag{9}$$

where $\bar{a}$ is the effective crack length, A_c is the area of a single cell (given previously), n_{DB} is the number of debonded cells counted in the x-ray image, and w is the specimen width. It should be noted that the cells in the center cut-out area and those cells debonded by the starter crack were also counted as debonded cells and used in calculating n_{DB}.

After completion of all the test runs, the inner facesheet was completely separated from the remaining bonded core and the failure surface was examined visually.

Results

The primary variables considered in this study were specimen orientation (transverse versus longitudinal) and test temperature. The impact of these variables on specimen stiffness, strain-energy release rate, crack growth, and the fracture surface will be considered herein.

Stiffness

Review of the data in Table 1 clearly indicates that the facesheet stiffness was a function of both orientation and temperature. Orientation was the biggest factor with a difference in stiffness between longitudinal and transverse directions on the order of 60%. Both facesheets, regardless of orientation, exhibited an increase in stiffness with a decrease in temperature. This difference was approximately 7% for both facesheets.

In comparison to many commercial systems [1] that can have relative densities in the range of 0.2 to 0.3, the relative density (Eq. (1)) of the core was quite low. Correspondingly, the in-plane and out-of-plane stiffness, as given by Eq.s (2) and (3), respectively, were also low, compared to many commercial systems.

Strain-Energy Release Rate

The critical strain-energy release rate (Eq. (8)) was found for both orientations and test temperatures. In order to characterize the critical strain-energy release rate, mean values were computed by using all the data over the entire range of effective crack length.

Room Temperature

The room temperature data, Fig. 9, indicates that there was no appreciable difference between the mean values of the longitudinal and transverse data. However, compared to the longitudinal orientation, the transverse orientation did result in a higher degree of data scatter.

Cryogenic Temperature

As with the room temperature data, the cryogenic temperature data, Fig. 10, indicates that there is no appreciable difference between the mean values of the longitudinal and transverse data. The degree of scatter did not appear to differ greatly for the different specimen orientations.

Combined Data

Both data sets, Figs. 9 and 10, were combined into one plot, Fig. 11, to illustrate the overall toughness trend with temperature. The mean values of G_c, were computed to be 356 J/m^2 and 163 J/m^2 for the cryogenic and room temperature data, respectively. This change in G_c with temperature represents a two-fold increase in G_c for a decrease in test temperature from 23^{0}C to –196^{0}C.

Crack Growth and the Fracture Surface

The x-ray images for most specimens, as illustrated by the typical data of Fig. 8, showed relatively stable crack growth as a function of the load. However, in some cases the crack front was not uniform and the debonded region was irregular. In all cases, Eq. (9) was used to calculate the effective crack length.

For all cases, regardless of test temperature or specimen orientation, the post-test examination of the fracture surface showed that failure always occurred along the core-to-adhesive bond line. The core separated cleanly from the facesheet, and the adhesive remained bonded to the inner facesheet.

Summary and Concluding Remarks

The in-plane stiffness of the composite facesheets was a strong function of specimen orientation and a weak function of test temperature. In general, the stiffness of the facesheets increased with a decrease in temperature. Therefore it is expected that the bending stiffness of the entire test specimen would be a function of facesheet orientation and exhibit an increase as test temperature decreases.

Examining the strain-energy release rate results from the current study of sandwich material, it was determined that G_c was independent of specimen orientation regardless of test temperature. It is significant, however, that G_c increased with a decrease

in temperature. In general, the G_c data was insensitive to changes in crack length.

The test apparatus and associated experimental methods developed in this study provide a novel approach to measuring the toughness of the facesheet-to-core bond and simulating the loading due to internal, core pressure. The primary experimental difficulties associated with this test method are related to the measurement of crack length. Further development may lead to a more precise, in-situ means of crack-growth measurement for a specimen immersed in cryogenic fluid.

Acknowledgements

The authors wish to acknowledge Mr. Ed Townsley, Mr. Scott Young, and Dr. Ed Glaessgen of NASA Langley Research Center for their invaluable contributions to the test program.

References

1. Gibson, L.J. and M.F. Ashby, *Cellular Solids, Structure and Properties*. Second ed. Cambridge Solid State Science Series. 1997, Cambridge: Cambridge University Press.

2. Robinson, M.J., *Composite Cryogenic Propellant Tank Development*. in *35th Structures, Structural Dynamics, and Materials Conference*. 1994, Hilton Head, South Carolina.

3. Robinson, M.J., *Composite Structures on the DC-XA Reusable Launch Vehicle*. in *28th International SAMPE*. 1996, Seattle, Washington.

4. NASA, Final Report of the X-33 Liquid Hydrogen Tank Test Investigation Team, George C. Marshall Space Flight Center, Huntsville, NASA Report, 2000, May, http://x33.msfc.nasa.gov/index.html

5. Aoki, T., et al., *Mechanical Performance of CF/Polymer Composite Laminates Under Cryogenic Conditions*. in *41st Structures, Structural Dynamics, and Materials Conference*. 2000, Atlanta, GA: American Institute of Aeronautics and Astronautics.

6. Donaldson, S.L. and R.Y. Kim, *Interlaminar Fracture of Carbon Fiber Reinforced Epoxy and Bismaleimide Composites at Cryogenic Temperatures*. in *American Society of Composites, 15th Technical Meeting*. 2000, College Station, TX: American Society of Composites.

7. Berry, J.P., *Determination of Fracture Energies by the Cleavage Technique*. Journal of Applied Physics, 1963. **34**(No. 1): p. 62-68.

8. Cantwell, W.F. and P. Davies, *A test technique for assessing core-skin adhesion in composite sandwich structures*. Journal of Material Science Letters, 1994. **13**: p. 203-205.

9. O' Brien, T.K. and R.H. Martin, *Round Robin Testing for Mode I Interlaminar Fracture Toughness of Composite Materials*. Journal of Composites Technology & Research, 1993. **15**(4): p. 269-281.

Outer Face Sheet, t=0.86mm [65/0/-65/90/-65/0/65]

Inner Face Sheet, t=1.78mm $[45/90_3/-45/0_3/-45/90_3/45]$

Figure 1. Facesheet push-off test specimen schematic.

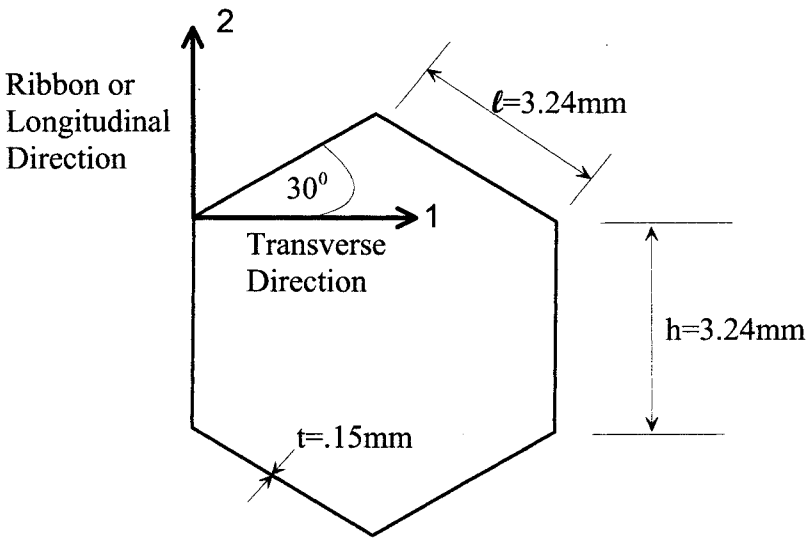

Figure 2. Honeycomb core cell cross-sectional schematic and coordinate system.

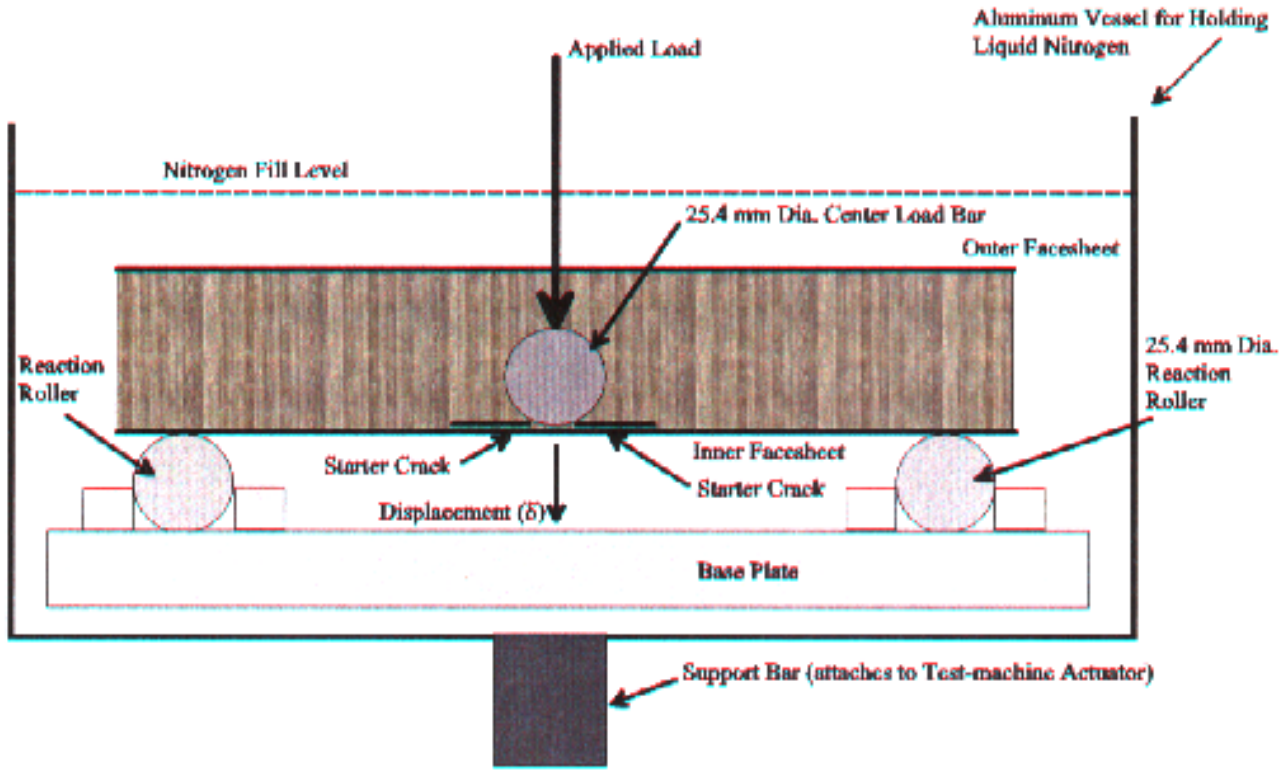

Figure 3. Facesheet push-off test fixture and specimen schematic.

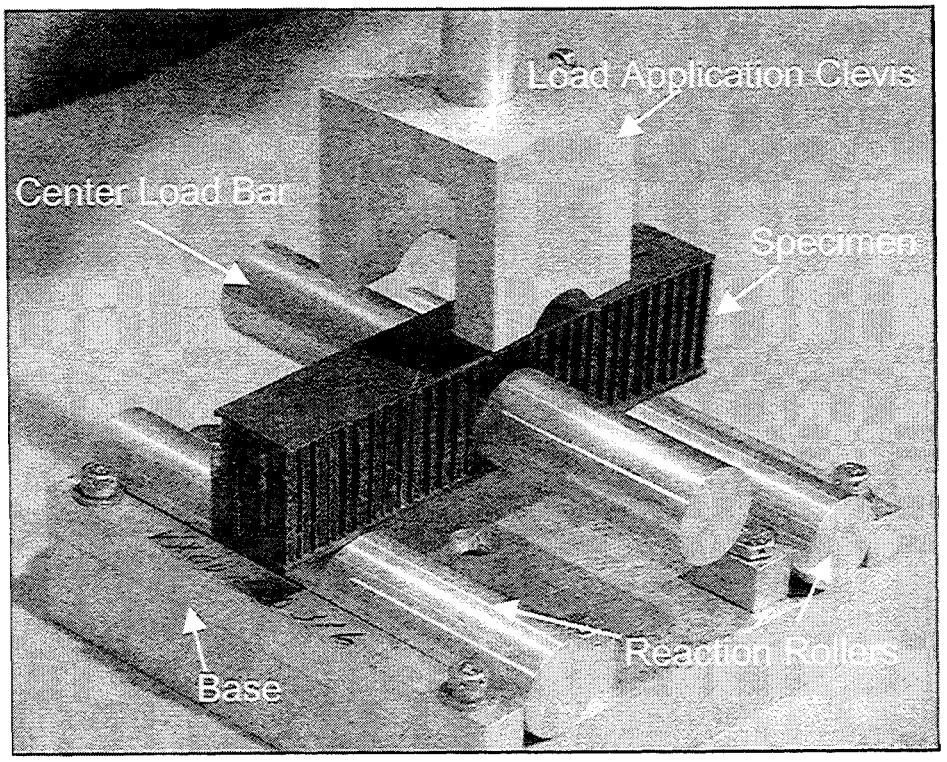

Figure 4. Facesheet push-off test fixture and specimen.

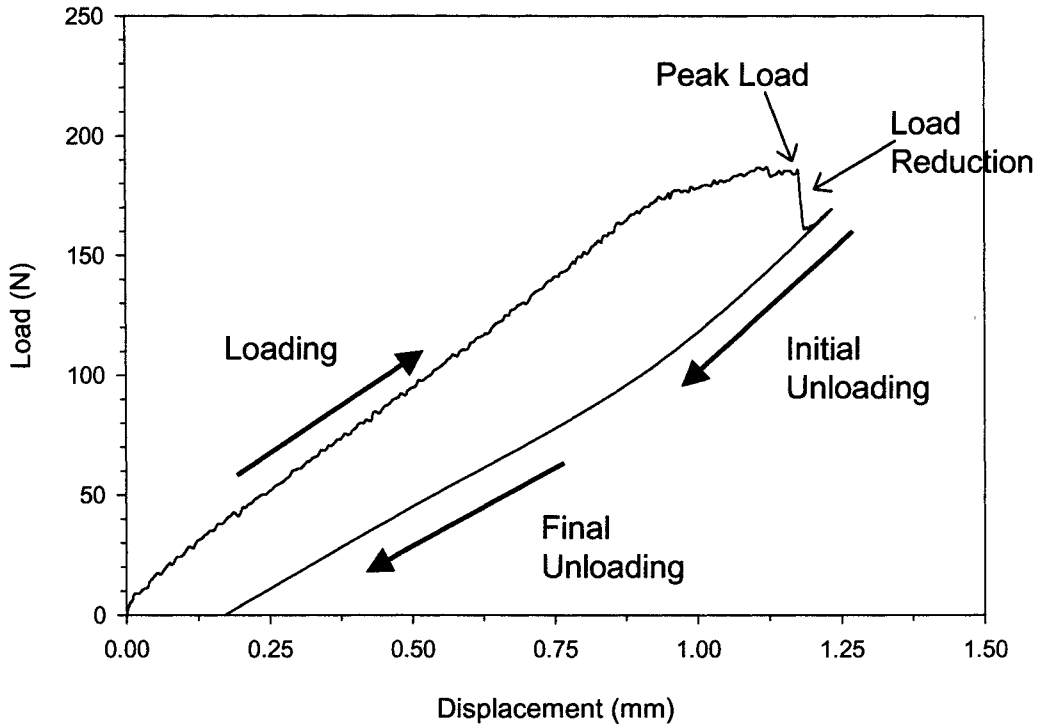

Figure 5. Typical load versus displacement plot showing definition of each aspect of the curve.

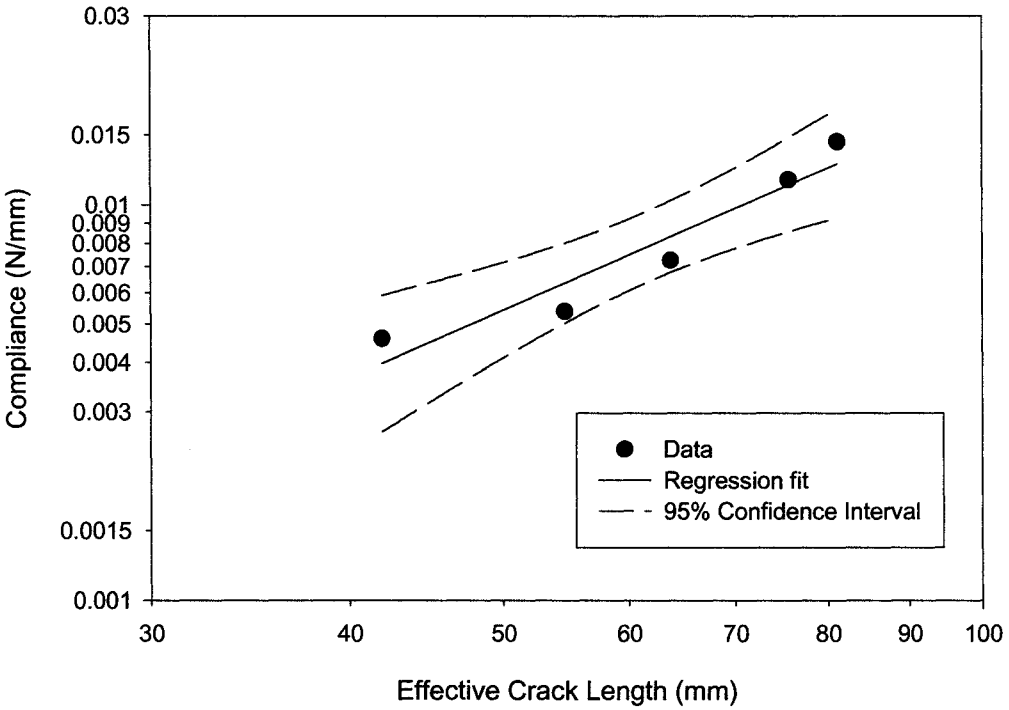

Figure 6. Typical computed compliance-versus-measured effective crack length data

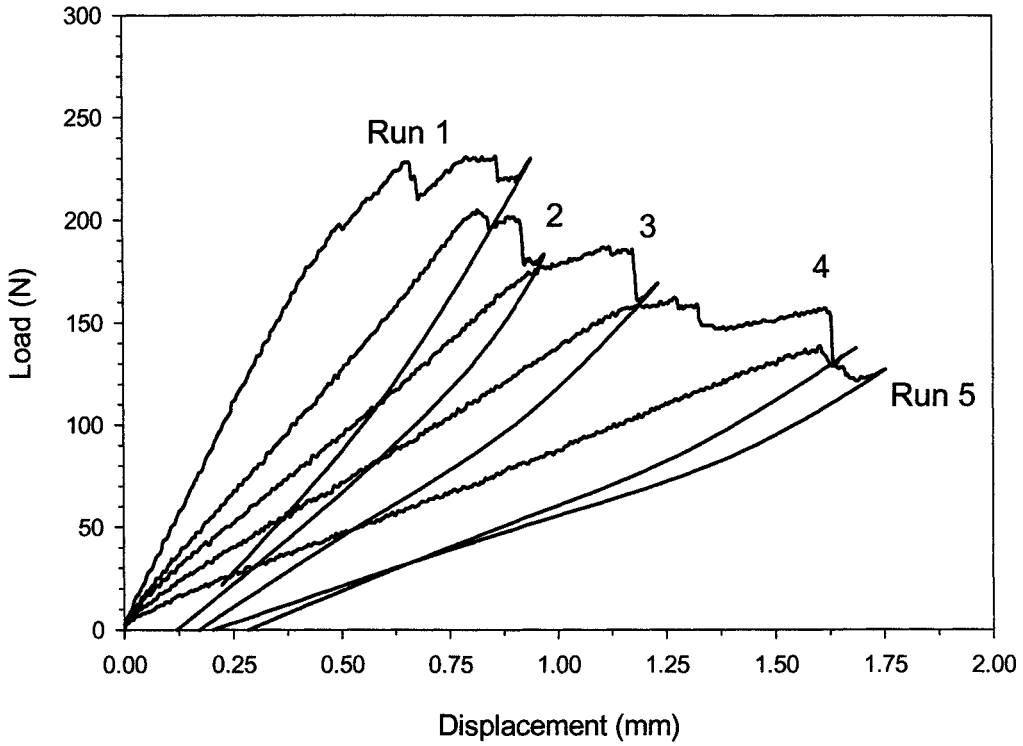

Figure 7. Load-versus-displacement plot showing 5 runs on the same specimen at room temperature.

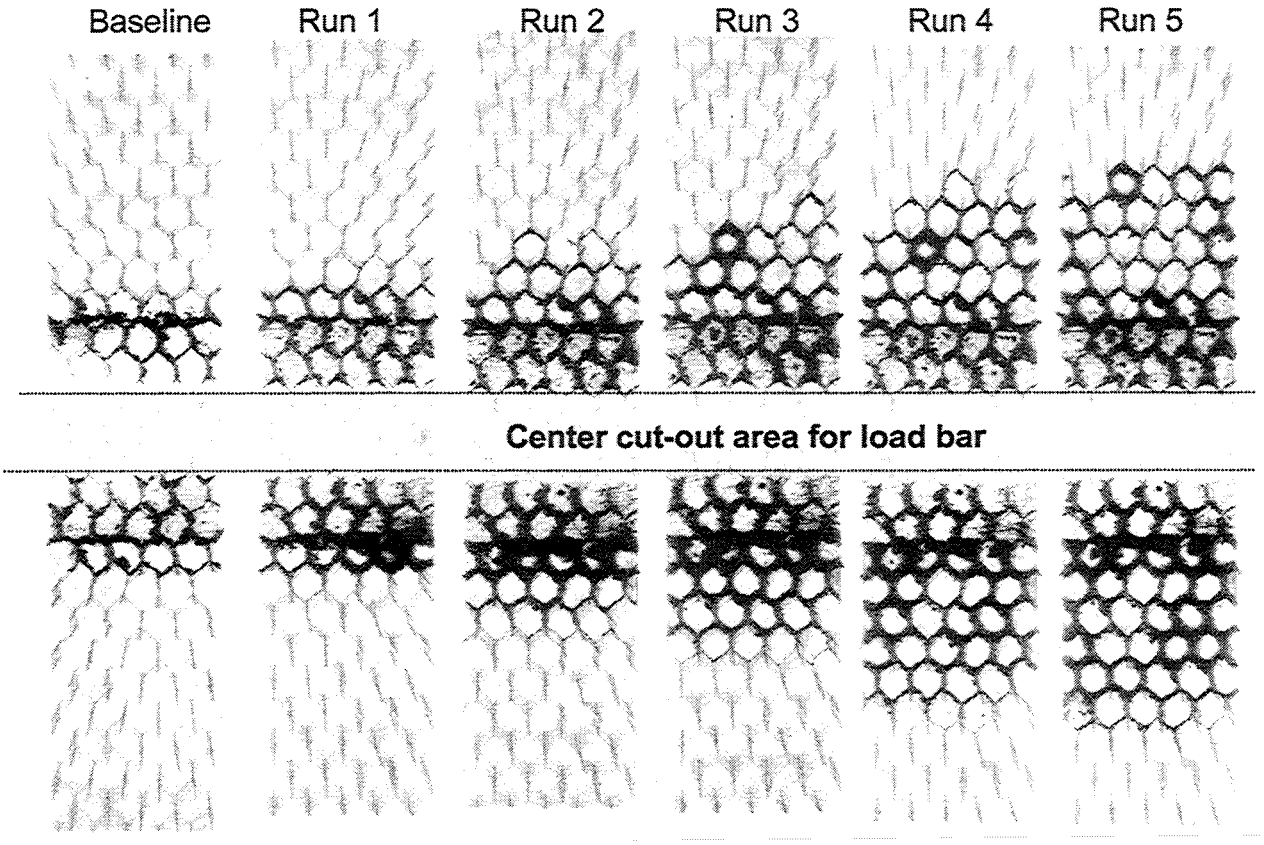

Figure 8. X-ray images of typical test specimen showing increase in debonded cells (dark regions) during loading. Corresponds to load-displacement plot of Fig. 7.

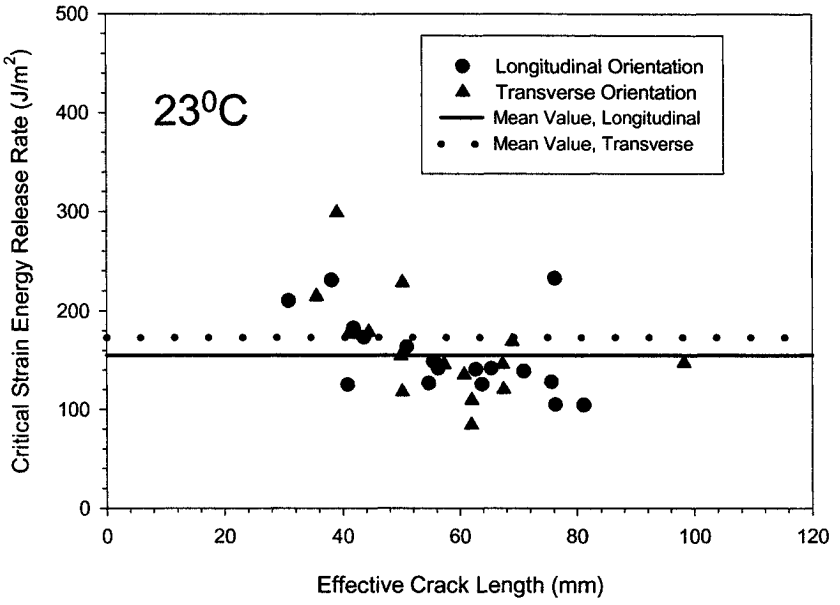

Figure 9. Effects of specimen orientation on sandwich toughness at room temperature.

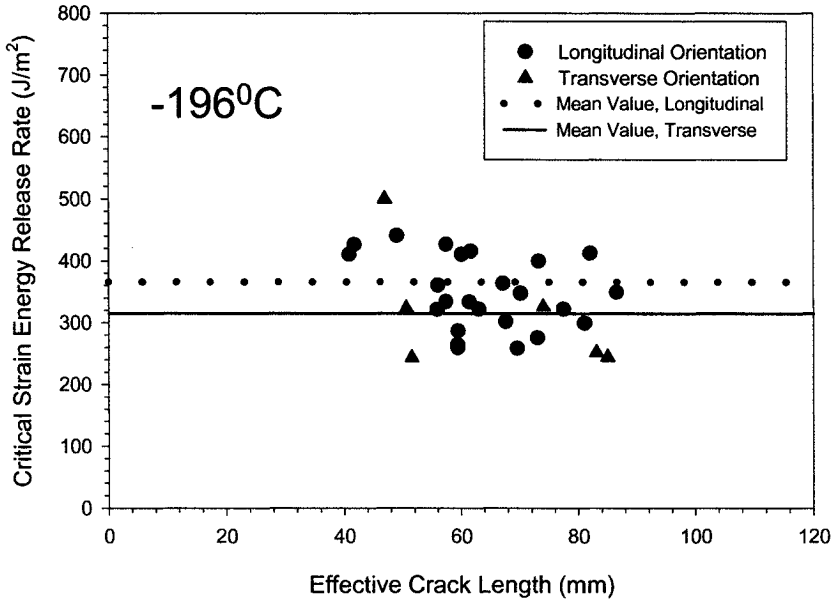

Figure 10. Effects of specimen orientation on sandwich toughness at cryogenic temperature.

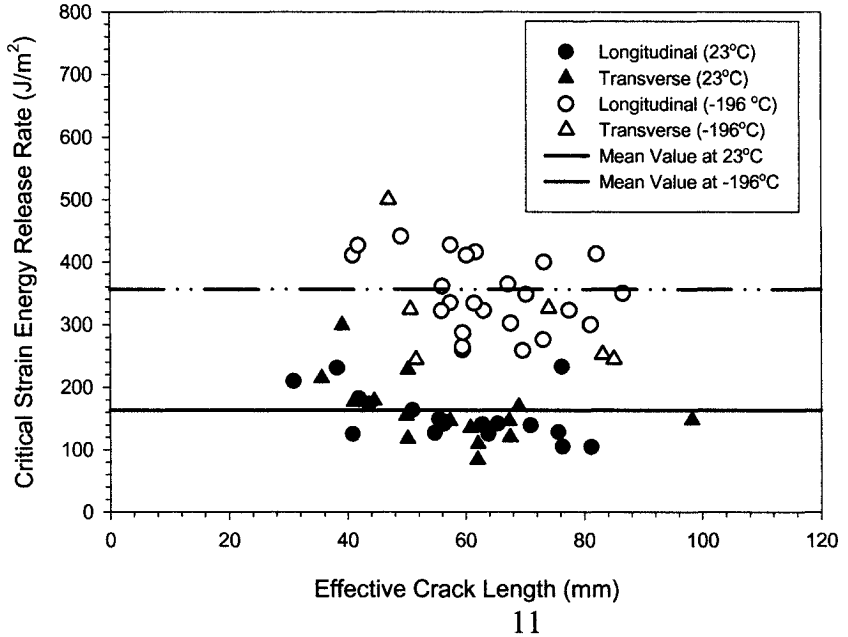

Figure 11. Effects of test temperature on sandwich toughness for all specimen orientations and temperatures.